

# Nonequilibrium critical dynamics in inhomogeneous systems

Michel Pleimling<sup>1</sup> and Ferenc Iglói<sup>2,3</sup>

<sup>1</sup>*Institut für Theoretische Physik I, Universität Erlangen-Nürnberg, D-91058 Erlangen, Germany*

<sup>2</sup>*Research Institute for Solid State Physics and Optics, H-1525 Budapest, P.O.Box 49, Hungary*

<sup>3</sup>*Institute of Theoretical Physics, Szeged University, H-6720 Szeged, Hungary*

(Dated: June 17, 2018)

We study nonequilibrium dynamical properties of inhomogeneous systems, in particular at a free surface or at a defect plane. Thereby we consider nonconserved (model-A) dynamics of a system which is prepared in the high-temperature phase and quenched into the critical point. Using Monte Carlo simulations we measure single spin relaxation and autocorrelations, as well as manifold autocorrelations and persistence. We show that, depending on the decay of critical static correlations, the short time dynamics can be of two kinds. For slow decay of local correlations the usual domain growth process takes place with non-stationary and algebraic dynamical correlations. If, however, the local correlations decay sufficiently rapidly we have the so called cluster dissolution scenario, in which case short time dynamical correlations are stationary and have a universal stretched exponential form. This latter phenomenon takes place in the surface of the three-dimensional Ising model and should be observable in real ferromagnets.

## I. INTRODUCTION

To characterize the dynamical universality class of a critical system at equilibrium it is enough to provide the value of the dynamical exponent,  $z$ , which generally depends on the local dynamics, conservation laws and symmetries.<sup>1</sup> In a nonequilibrium system, which is prepared by quenching it from the high-temperature initial state to the critical point, new nonequilibrium critical exponents have to be defined.<sup>2,3</sup> The reason of this is the broken time translation invariance due to a discontinuity at the time horizon ("time-surface"). Since at the critical point there is no characteristic time-scale the nonequilibrium preparation has a long-lasting effect, which has two important consequences. First, the dynamical correlations, such as the single spin autocorrelation function,  $C(t, s)$ , are generally non-stationary. They depend on both the preparation or waiting time,  $s$ , and the observation time,  $t$ . The second effect is the appearance of a new nonequilibrium critical exponent,  $\lambda$ , which is used to describe the long-time asymptotic,  $t \gg s$ , of the autocorrelation function as  $C(t, s) \sim t^{-\lambda/z}$ .<sup>3</sup>

Another, and related process of nonequilibrium dynamics is the relaxation of the magnetization, if in the initial state there is a small, non-vanishing value of  $m_i$ . For short times the magnetization has a power-law dependence:  $m(t) \simeq m_i t^\theta$ , with the initial slip exponent  $\theta$  which satisfies the scaling relation:  $\lambda = d - \theta z$ .<sup>2,4</sup> Here  $d$  is the spatial dimension of the system. In mean-field theory  $\theta = 0$ , whereas in real system generally  $\theta > 0$ . Thus due to fluctuations the order is increasing in the early time regime. This phenomenon is related to the fact that in the initial state there are no long-range correlations, thus the systems is mean-field like. Since the actual critical temperature of the system,  $T_c$ , is lower than the critical temperature of the mean-field model,  $T_c(mf) > T_c$ , in the early time-steps there is an effective coarsening process, during which the magnetization is increasing. The nonequilibrium magnetization with

$m_i < 1$ , however, can not exceed the value obtained with  $m_i = 1$ , when from the ordered initial state the magnetization decreases as  $m(t) \sim t^{-x/z}$ , where  $x$  is the anomalous dimension of the magnetization. This critical parameter is defined through the asymptotic decay of the equilibrium, equal-time correlation function at the critical point:  $\langle \sigma_i(t) \sigma_j(t) \rangle \sim |i - j|^{-2x}$  and satisfies the scaling relation:  $x = \beta/\nu$ , with  $\beta$  and  $\nu$  being the usual static magnetization and correlation length exponents, respectively. From the previous reasoning we obtain for the border of the short-time regime,  $t_i$ , as  $t_i \sim m_i^{-z/x_i}$ , where  $x_i = \theta z + x$  is the anomalous dimension of the initial magnetization. Note that the nonequilibrium time-scale,  $t_i$ , diverges as  $m_i \rightarrow 0$ .

Besides single spin autocorrelations one often considers the dynamics of extended objects, such as the order-parameter of the whole sample (global autocorrelations) or that of a manifold<sup>5</sup> with dimension  $d' < d$ . In the asymptotic regime  $t \gg s$  the manifold autocorrelation function displays an algebraic decay<sup>5</sup>:  $G(t) \sim t^{-\lambda'/z}$  with  $\lambda' = \lambda - d'$ . Still another dynamical quantity is represented by the persistence,  $P_{pr}(t)$ , which measures the probability that the order-parameter associated either to a single spin, or to a manifold, or to the whole sample has not changed sign within time  $t$ .<sup>6</sup> Among others, persistence is related to the properties of the given autocorrelation function and for global and manifold persistence it has often a power-law dependence:  $P_{pr}(t) \sim t^{-\Theta_{pr}}$ , where  $\Theta_{pr}$  is a new nonequilibrium exponent.<sup>7</sup> Only for global persistence and for a Markovian process can  $\Theta_{pr}$  be expressed by other known exponents.<sup>7</sup>

The dynamical critical behavior, as outlined above, refers to the bulk of a homogeneous system in the thermodynamic limit. Real materials, however, are bounded by surfaces and many nonequilibrium processes (thermalization, transfer of heat, etc.) are very intensive at the surface. At a free boundary layer the order is weaker than in the bulk due to missing bonds and correlations between two surface sites,  $i_1, j_1$ :  $\langle \sigma_{i_1}(t) \sigma_{j_1}(t) \rangle \sim |i_1 - j_1|^{-2x_1}$  in-

volve a new scaling dimension,  $x_1 > x$ .<sup>11,12,13,14</sup> This satisfies the scaling relation:  $x_1 = \beta_1/\nu$ , with  $\beta_1$  being the surface magnetization exponent. Note that there is an analogy between spatial and temporal surfaces, where translational invariance in space and in time, respectively, is broken. Similarly the scaling dimensions,  $x_1$  and  $x_i$ , respectively, play analogous roles. According to field-theoretical investigations<sup>15</sup> no new dynamical critical exponent should be introduced at the surface:  $z$  and  $x_i$  remain unchanged whereas  $\theta_1$  and  $\lambda_1$ , as defined on surface spins, can again be expressed by the known exponents, including  $x_1$ .<sup>16,17</sup>

We note that besides a free surface there exist other types of inhomogeneities, such as a localized or an extended defect plane, near which scaling of the local magnetization is different from that in the bulk. Correlations between two sites at the defect plane,  $i_l, j_l$  are asymptotically given at the critical point by  $\langle \sigma_{i_l}(t) \sigma_{j_l}(t) \rangle \sim |i_l - j_l|^{-2x_l}$ , which involves a new static (local) exponent  $x_l \neq x$ .<sup>13</sup> In an inhomogeneous system it can be found in many cases that  $x_l > x_i$ , thus the spatial surface or interface is more disordered than the "temporal surface". This happens for example at the ordinary surface transition of the three-dimensional Ising model, with  $x_1 = 1.26$  and  $x_i = 0.74$ , and should be realized in real magnets, too. Nonequilibrium dynamical critical behavior of systems with  $x_l > x_i$  is expected to be different from that with  $x_l < x_i$ . In the latter case traditional domain growth (DG) scenario should hold. On the other hand in the former case critical relaxation is more effective than the nonequilibrium growth, therefore no new domains are created in the surface or interface region. The dynamical process is dominated by rare clusters with correlated sites, and the nonequilibrium dynamics is realized through cluster dissolution (CD). The CD process can be seen also for the surface manifold autocorrelation function, provided  $d' - x_l - x < 0$ .<sup>18</sup>

Our aim in the present paper is to study in detail the nonequilibrium dynamical critical behavior in inhomogeneous systems, in particular at a free surface or at defect planes. Here we restrict ourselves to nonconserved (model-A) dynamics.<sup>1</sup> We use scaling theory and perform extensive Monte Carlo simulations. We clarify the properties of the nonequilibrium dynamics in the DG and CD regimes. A short account of our results obtained at a free surface has been announced in a Letter.<sup>18</sup>

Our paper is organized as follows. In Sec. 2 we start with the presentation of a phenomenological picture based on scaling theory. Sec. 3 contains our numerical results on local magnetization relaxation and autocorrelations i) at free surfaces in the two- and three-dimensional Ising models, ii) at an extended surface defect in the two-dimensional Ising model (Hilhorst-van Leeuwen (HvL) model),<sup>19</sup> and iii) at an internal defect line in the two-dimensional Ising model (Bariev model).<sup>20</sup> We also consider iv) surface manifold autocorrelations and persistence. In Sec. 4 we close our paper by a discussion.

## II. SCALING THEORY OF NONEQUILIBRIUM DYNAMICS IN INHOMOGENEOUS SYSTEMS

We consider a  $d$ -dimensional system having a free surface or a defect plane, the distance of it being denoted by  $y$ . (In the following we will refer to that plane as a *surface* and the local scaling dimension will be called  $x_l$ , so that  $x_l = x_1$  at a free surface.) From the high-temperature phase,  $T > T_c$ , we quench the system to its critical temperature and study different physical quantities (magnetization, single spin autocorrelation, manifold autocorrelation) as a function of the waiting time,  $s$ , and the observation time,  $t$ , both measured from the time of the quench. We start our analysis with the relaxation of the magnetization.

### A. Relaxation of the magnetization

In this case the system is prepared with a small initial magnetization,  $m_i > 0$ , and the local magnetization  $m = \langle \sigma_y(t) \rangle \equiv m(y, t, m_i)$  is measured at the critical temperature. Here  $\sigma_y(t)$  is the operator of the local magnetization. Under a scaling transformation,  $l \rightarrow l/b$ , when length,  $l$ , is rescaled by a factor,  $b > 1$ , the magnetization behaves as:

$$m(y, t, m_i) = b^{-x} m(y/b, t/b^z, m_i b^{x_i}). \quad (1)$$

Here  $x_i$  is the new, nonequilibrium scaling dimension of the initial magnetization, as introduced in the previous section. Taking in Eq.(1)  $b = t^{1/z}$ , we arrive to:

$$m(y, t, m_i) = t^{-x/z} \tilde{m}(y/t^{1/z}, m_i t^{x_i/z}), \quad (2)$$

in which the scaling function,  $\tilde{m}(r, \mu)$ , behaves differently in the bulk,  $r \rightarrow \infty$ , and at the surface,  $r \rightarrow 0$ , respectively.

#### 1. Bulk behavior

In the bulk of the system we have by definition  $\lim_{r \rightarrow \infty} \tilde{m}(r, \mu) = \tilde{m}_b(\mu)$ , and the bulk scaling function  $\tilde{m}_b(\mu)$  has a cross-over:

$$\tilde{m}_b(\mu) = \begin{cases} \sim \mu, & \mu \ll 1 \\ \text{const}, & \mu \gg 1 \end{cases} \quad (3)$$

For short times,  $t < t_i \sim m_i^{-z/x_i}$ , the magnetization increases as  $m(t) \sim t^\theta$ , with  $\theta = (x_i - x)/z$ . For longer times, however, the magnetization follows the equilibrium decay,  $m(t) \sim t^{-x/z}$ . We note that the short-time behavior of the magnetization is the result of two different processes. Due to nonequilibrium domain growth the magnetization increases as  $t^{x_i/z}$ , whereas critical relaxation acts to reduce its value by  $t^{-x/z}$ .

## 2. Surface behavior

In order to understand the concept of surface critical behavior we start with the equilibrium magnetization,  $m_{\text{eq}}(y, t, \delta)$ , where  $\delta = (T_c - T)/T_c$  is the reduced critical temperature. The scaling transformation now reads as:

$$m_{\text{eq}}(y, t, \delta) = b^{-x} m_{\text{eq}}(y/b, t/b^z, \delta b^{1/\nu}). \quad (4)$$

We consider first the *static* behavior with  $t = 0$ , set the length-scale to  $b = \delta^{-\nu}$  and obtain  $m_{\text{eq}}(y, t = 0, \delta) = \delta^{x\nu} \tilde{m}_{\text{eq}}(y\delta^\nu)$ . Here we notice the temperature dependence of the bulk magnetization:  $m_{\text{eq}}^b \sim \delta^\beta$ , with a critical exponent  $\beta = x\nu$  and with the scaling function:  $\lim_{\tilde{r} \rightarrow \infty} \tilde{m}_{\text{eq}}(\tilde{r}) = \text{const}$ . By definition the magnetization at the surface behaves as:  $m_{\text{eq}}^s \sim \delta^{\beta_l}$  with  $\beta_l = x_l\nu$ . This is compatible with the above scaling result provided the scaling function for a small argument (short distance) behaves as:  $\lim_{\tilde{r} \rightarrow 0} \tilde{m}_{\text{eq}}(\tilde{r}) \sim \tilde{r}^{x_l - x}$ . Now considering the equilibrium *dynamical behavior* at the critical point we set in Eq.(4)  $\delta = 0$  and  $b = t^{1/z}$ . Repeating the previous reasoning we obtain for the magnetization in the surface region  $m_{\text{eq}}(y, t) = t^{-x/z} \tilde{m}_{\text{eq}}(r) \sim t^{-x/z} r^{x_l - x}$ ,  $r \ll 1$ , which can be obtained from the short-distance expansion in field-theoretical calculations.<sup>12</sup> Note that starting from the bulk order is decreasing towards the surface for  $x_l > x$ . In nonequilibrium relaxation two processes have to be taken into account close to a surface: the magnetization i) increases due to nonequilibrium domain growth and ii) decreases due to surface effects. Of course, the first process is of no importance when starting from a fully ordered state.<sup>21,22</sup> The relative strength of the two processes are given by the scaling dimensions  $x_i$  and  $x_l$ , respectively. Nonequilibrium dynamics is markedly different for  $x_i > x_l$ , which is the domain growth regime, and for  $x_i < x_l$ , which is the regime of cluster dissolution.

*a. Domain growth:  $x_i > x_l$*  In this case bulk nonequilibrium order penetrates into the surface region, in which, as time goes on, new domains are formed. Therefore short distance expansion of the magnetization stays valid, yielding for small  $r$  the following expression for the scaling function  $\tilde{m}(r, \mu)$  given in Eq.(2):

$$\lim_{r \rightarrow 0} \tilde{m}(r, \mu) = r^{x_l - x} \tilde{m}_l(\mu), \quad x_i > x_l. \quad (5)$$

Here  $\tilde{m}_l(\mu)$  has the same limiting  $\mu$ -dependence as  $\tilde{m}_b(\mu)$  in Eq.(3). Thus we have in the short-time limit,  $t < t_i \sim m_i^{-z/x_i}$ ,  $m_l(t) \sim t^{\theta_l}$ , with  $\theta_l = \theta - (x_l - x)/z = (x_i - x_l)/z$ . Thus the initial slip exponent at the surface in the DG regime can be expressed by known exponents.<sup>16</sup>

*b. Cluster dissolution:  $x_i < x_l$*  In this case, for short times nonequilibrium order can not penetrate into the surface region and therefore no new domains are formed there. In contrary the initially existing ordered clusters are diluted and the initial relaxation has a fast, non-algebraic dependence. Evidently the short distance expansion is not valid here. Analyzing the CD process we have determined in the Appendix the small  $r$  behavior

of the scaling function,  $\tilde{m}(r, \mu)$ . It is given in a stretched exponential form:

$$\lim_{r \rightarrow 0} \tilde{m}(r, \mu) \sim \exp(-Cr^\kappa), \quad x_i < x_l, \quad (6)$$

with a universal power:

$$\kappa = \frac{(x_l - x_i)d}{d - 1}, \quad (7)$$

If  $\kappa/z > 1$ , as argued in the Appendix, the functional form in Eq.(6) is pure exponential. This time dependence is valid for  $t < t'_i \sim |\ln m_i|^{z/\kappa}$ , for larger times one goes over to the DG regime with the decay in Eq.(5).

## B. Single spin autocorrelation function

The nonequilibrium autocorrelation function is defined by  $C(y, t, s) = \langle \sigma_y(t) \sigma_y(s) \rangle$  and in the prepared state there is no initial magnetization. From the scaling transformation of the autocorrelation function:

$$C(y, t, s) = b^{-2x} C(y/b, t/b^z, s/b^z) \quad (8)$$

we obtain with  $b = t^{1/z}$ :

$$C(y, t, s) = t^{-2x/z} \tilde{C}(y/t^{1/z}, s/t). \quad (9)$$

In the following we analyze the scaling function,  $\tilde{C}(r, \tau)$ ,  $\tau \leq 1$ , in the different limits.

### 1. Bulk behavior

The scaling function in the bulk,  $\lim_{r \rightarrow \infty} \tilde{C}(r, \tau) = \tilde{C}_b(\tau)$ , has the asymptotic behavior:

$$\lim_{\tau \rightarrow 0} \tilde{C}_b(\tau) \sim \tau^{(d - x_i - x)/z}. \quad (10)$$

So that for  $t \gg s$  we have  $C_b(t) \sim t^{-\lambda/z}$ , with the bulk autocorrelation exponent:  $\lambda = d - x_i + x$ .

### 2. Surface behavior

As for the magnetization relaxation we have to discriminate between two regimes: the DG and the CD dynamics, for  $x_i > x_l$  and  $x_i < x_l$ , respectively.

*a. Domain growth:  $x_i > x_l$*  In this case domain growth takes place in the surface region, too. Therefore for small  $r$  we can separate the  $r$ -dependence from the scaling function in Eq.(9), leading to:

$$\lim_{r \rightarrow 0} \tilde{C}(r, \tau) = r^{2(x_l - x)} \tilde{C}_l(\tau), \quad x_i > x_l. \quad (11)$$

The small  $\tau$  dependence of the scaling function  $\tilde{C}_l(\tau)$  is the same as in Eq.(10) for the bulk quantity:  $\tilde{C}_l(\tau) \sim \tau^{(d - x_i - x)/z}$ . Consequently in the limit  $t \gg s$  we have for the surface autocorrelation function  $C_l(t) \sim t^{-\lambda_l/z}$ , with the surface autocorrelation exponent:  $\lambda_l = \lambda + 2(x_l - x) = d - x_i - x + 2x_l$ .<sup>16</sup>

*b. Cluster dissolution:  $x_i < x_l$*  In this case typically no new domains are formed in the surface region. The autocorrelation function of the system is therefore dominated by such rare regions in which at preparation there is an ordered cluster. The probability of the existence of such a region is very small as it decreases exponentially with its volume. The relaxation time, however, associated to such a cluster is very large, it is the exponential function of the typical size of an interface in this cluster. Combining these two effects we arrive to a stretched exponential dependence, as described in the Appendix. Since the starting cluster structure does not depend on the waiting time the surface autocorrelation function for a small  $t - s \ll s$  is stationary. In this case both  $r \rightarrow 0$  and  $1 - \tau \rightarrow 0$ , so that the appropriate scaling combination is  $\rho = (1 - \tau)^{1/z}/r$ . In terms of this the surface autocorrelation function in the CD regime is

$$C_l(t) \sim \exp(-C'(t-s)^{\kappa/z}) \quad (12)$$

for  $\kappa/z < 1$ , with the exponent  $\kappa$  given in Eq. (7), whereas for  $\kappa/z > 1$  the functional form in Eq. (12) is pure exponential.

### C. Manifold autocorrelations

Here we consider a  $d'$  dimensional manifold,  $\mathcal{M}$ , which is located at a distance  $y$  from the surface. The manifold order-parameter is the sum of the individual operators,  $S_y = \sum_{i \in \mathcal{M}} \sigma_y(i)$ , and the manifold autocorrelation function is defined by  $G(y, t, s) = \langle S_y(t) S_y(s) \rangle$ . This quantity, as well as manifold persistence, has been introduced and studied in the bulk of the system by Majumdar and Bray.<sup>5</sup> First, we consider the equal-time autocorrelation function,  $G(y, t, t) = \langle \sum_{i \in \mathcal{M}} \sigma_y(i) \sum_{j \in \mathcal{M}} \sigma_y(j) \rangle$ , and note that in the disordered initial state at  $t = s = 0$  it is zero, since  $S_y = 0$ . As time goes on correlations between sites within the correlated domain of linear size,  $\xi \sim t^{1/z}$ , are built, so that for a bulk manifold contribution of terms with alternating signs will lead to  $\langle \sigma_y(i) \sum_{j \in \mathcal{M}} \sigma_y(j) \rangle \sim t^{-2x/z}$  and therefore  $G_b(t, t) = \lim_{y \rightarrow \infty} G(y, t, t) \sim t^{(d'-2x)/z}$ , provided  $d' > 2x$ . If, however,  $d' < 2x$ , since the equal-time autocorrelation function can not decrease,  $G_b(t, t)$  will approach a finite limiting value within a characteristic (microscopic) time. In this case  $G_b(t, t)$  being independent of the waiting time the manifold autocorrelation function is stationary,  $G_b(t, s) = G_b(t - s)$ . This type of results are in complete agreement with the mean-field and scaling results of Ref. 5.

The above observations can be cast into a scaling relation for the manifold autocorrelation function as:

$$G(y, t, s) = t^{(d'-2x)/z} \tilde{G}(y/t^{1/z}, s/t), \quad (13)$$

in which the scaling function,  $\tilde{G}(r, \tau)$ , has different analyticity properties in the different regimes.

#### 1. Bulk behavior

The scaling function in the bulk is denoted as  $\lim_{r \rightarrow \infty} \tilde{G}(r, \tau) = \tilde{G}_b(\tau)$ .

*a. Non-stationary regime:  $d' > 2x$*  Here  $\tilde{G}_b(\tau)$  is analytic for  $\tau \geq 1$  and has the limiting behavior:

$$\lim_{\tau \rightarrow 0} \tilde{G}_b(\tau) \sim \tau^{(d-x_i-x)/z}. \quad (14)$$

So that for  $t \gg s$  we have  $G_b(t) \sim t^{-\lambda'/z}$ , with the bulk manifold autocorrelation exponent:  $\lambda' = d - d' - x_i + x$ . Note that for the global autocorrelation function with  $d' = d$  the decay exponent,  $\lambda'/z$ , is just the initial slip exponent,  $\theta$ .

*b. Stationary regime:  $d' < 2x$*  In this regime the scaling function is non-analytic at  $\tau = 1$  and given for  $1 - \tau \ll 1$  as:

$$\tilde{G}_b(\tau) \sim (1 - \tau + \tau_0)^{(d'-2x)/z}, \quad (15)$$

where  $\tau_0$  is related to the microscopic time-scale until which  $G_b(t, t)$  reaches its limiting value. In the limit,  $1 - \tau \gg \tau_0$ , we combine Eq.(15) with (13) and obtain a stationary short-time behavior:

$$G_b(t, s) \sim (t - s)^{(d'-2x)/z}, \quad (16)$$

in complete agreement with Ref. 5.

#### 2. Surface behavior

Here we consider first the initial value of the manifold autocorrelations at the waiting time  $t = s$ , thus we have  $\tau = 1$ . For equal time operators the short distance expansion is expected to be the same as for the magnetization in Eq.(5) so that the scaling function behaves as:

$$\lim_{r \rightarrow 0} \tilde{G}(r, \tau = 1) \sim r^{x_l - x}. \quad (17)$$

Consequently the surface manifold autocorrelation function at the waiting time reads as:

$$G_l(t, t) \sim t^{(d'-x_l-x)/z}. \quad (18)$$

Thus, as for the bulk manifold, the time-dependence of  $G_l(t, t)$ , and thus the non-equilibrium dynamics has two different regimes. For  $d' > x_l + x$ , when  $G_l(t, t)$  is divergent for large  $t$  we are in the standard DG regime. On the contrary for  $d' < x_l + x$ , when  $G_l(t, t)$  approaches a finite limiting value within a microscopic time-scale the dynamics for  $t > s$  is of the CD type.

*a. Domain growth:  $d' > x_l + x$*  For  $t > s$  the manifold autocorrelation function has the same short distance expansion as the single spin autocorrelation function in Eq.(11), thus the scaling function,  $\tilde{G}(r, \tau)$ , for small  $r$  behaves as:

$$\lim_{r \rightarrow 0} \tilde{G}(r, \tau) = r^{2(x_l-x)} \tilde{G}_l(\tau), \quad d' > x_l + x. \quad (19)$$

Note that the form of the short distance expansion is radically changing for  $t > s$  in comparison with that for  $t = s$  in Eq.(17). The scaling function,  $\tilde{G}_l(\tau)$ , has the same small  $\tau$  dependence as its bulk counterpart in Eq.(14), thus  $\lim_{\tau \rightarrow 0} \tilde{G}_l(\tau) \sim \tau^{(d-x_i-x)/z}$ . As a final result for  $t \gg s$  the surface manifold autocorrelation function in the DG regime behaves as:  $G_l(t) \sim t^{-\lambda'_l/z}$ , with the surface manifold autocorrelation exponent:  $\lambda'_l = \lambda' + 2(x_l - x) = d - d' - x_i - x + 2x_l$ .

*b. Cluster dissolution:*  $d' < x_l + x$  In this case the correlated sites form isolated clusters and the dominant contribution of the manifold autocorrelation function is due to large, but rare clusters. The dilution of the clusters during the relaxation process for  $t > s$  is similar to that of the single spin autocorrelation function. The only difference is that here the creation of sites in the domain wall of ordered clusters goes on with time as  $t^{x_l-x}$ , which follows from the difference in the short distance expansions of  $G(r, \tau = 1)$  in Eq. (17) and that of  $G(r, \tau < 1)$  in Eq. (19). As for the single spin autocorrelation for short times,  $t - s \ll s$ , the manifold autocorrelation function is stationary. This means that as  $r \rightarrow 0$  and  $1 - \tau \rightarrow 0$  the appropriate scaling combination is  $\rho = (1 - \tau)^{1/z}/r$ , in terms of which the surface manifold autocorrelation function is given by

$$G_l(t) \sim \exp(-C''(t-s)^{\kappa'/z}) \quad (20)$$

for  $0 < \kappa'/z < 1$  with the exponent  $\kappa' = (x_l - x)d/(d-1)$ . If  $\kappa'/z > 1$  then the functional form in Eq.(20) is pure exponential.

Here we note that for manifold autocorrelations there is an analogy between the stationary regime in the bulk and the CD regime at the surface. The difference in the functional forms in Eqs.(16) and (20) is due to the relevant inhomogeneity in the latter case: bulk order can only in a very limited way penetrate into the surface region. Formally, in the bulk  $\kappa'$  should be replaced by zero and therefore the decay is algebraic, as given in Eq.(16).

#### D. Persistence of manifolds

Persistence of manifolds is given by the probability  $P_{pr}(t)$  that the manifold order-parameter,  $\langle S_y(t) \rangle$ , has not changed sign up to time  $t$ . The bulk manifold persistence has been analyzed by Majumdar and Bray<sup>5</sup> and here we shortly recapitulate their findings.

##### 1. Bulk behavior

In this case the functional form of persistence can be formally related to the manifold autocorrelation function at the waiting time, which according to Eq.(13) is given by  $G(t, t) \sim t^{-\zeta}$ , with  $\zeta = (2x - d')/z$ . In the actual analysis the theorem by Newell and Rosenblatt<sup>23</sup> is used in which the long time decay of the persistence

of a Gaussian stationary process is related to the asymptotic decay of its stationary autocorrelation function. For  $\zeta < 0$  the non-stationary correlator after rescaling and in  $\log t$  variable is transformed to a stationary one. From this persistence in  $t$  is obtained in a power-law form,  $P_{pr}(t) \sim t^{-\Theta_{pr}}$ , with a non-trivial exponent,  $\Theta_{pr}$ . For  $0 < \zeta$  the autocorrelation function in Eq.(16) is stationary and one can apply directly the theorem by Newell and Rosenblatt.<sup>23</sup> For  $0 < \zeta < 1$  persistence is in a stretched exponential form:  $P_{pr}(t) \sim \exp(-at^\zeta)$ , whereas for  $\zeta > 1$  it is pure exponential:  $P_{pr}(t) \sim \exp(-bt)$ .

##### 2. Surface behavior

Here we should distinguish between the DG and the CD regimes. In the DG regime having a nonstationary autocorrelation function persistence can be analyzed in a similar way as for the analogous regime in the bulk. In this way we obtain that for  $d' > x_l + x$ , the surface manifold persistence is of a power-law form,  $P_{pr}(t) \sim t^{-\Theta'_{pr}}$ . In the CD regime, with  $d' < x_l + x$ , the autocorrelation function is stationary in the short-time regime,  $t - s < s$ , but for longer times it becomes non-stationary. Since the dominant variation of persistence is related to the stationary part of the correlator it is natural to assume that persistence has the same type of stretched or pure exponential time dependence, as the autocorrelation function. Thus for  $0 < \kappa'/z < 1$ ,  $P_{pr}(t) \sim \exp(-at^{\kappa'/z})$ , whereas for  $\kappa'/z > 1$  we have  $P_{pr}(t) \sim \exp(-bt)$ .

### III. NUMERICAL RESULTS

We discuss in the following the nonequilibrium dynamical behavior of various inhomogeneous systems and confront the numerical results with the predictions coming from the scaling theory just presented. The models studied include semi-infinite Ising models in two and three dimensions, the Hilhorst-van Leeuwen model (i.e. two-dimensional semi-infinite Ising model with an extended surface defect) and Ising models with a ladder defect.

#### A. The models

##### 1. Semi-infinite Ising models

Static and dynamical properties of critical semi-infinite systems have been studied very intensively during the last thirty years<sup>11,12,14</sup>. The simplest of these models is the semi-infinite Ising model defined by the Hamiltonian

$$\mathcal{H} = -J_s \sum_{surface} \sigma_i \sigma_j - J_b \sum_{bulk} \sigma_i \sigma_j \quad (21)$$

where the spin located at site  $i$  takes on the values  $\sigma_i = \pm 1$ . The first sum in Eq. (21) is over nearest neighbor pairs of surface spins, whereas the second sum is over

TABLE I: Static and dynamic critical quantities of the two- and the three-dimensional Ising models.  $x$ : bulk scaling dimension,  $x_1$ : surface scaling dimension,  $x_i$ : scaling dimension of the initial magnetization,  $z$ : dynamical scaling exponent. OT: ordinary transition, SP: special transition point.

	$x$	$x_1$	$x_i$	$z$
$d = 2$	1/8	1/2	0.53	2.17
$d = 3$ , OT	0.516	1.26	0.74	2.04
$d = 3$ , SP	0.516	0.376	0.74	2.04

nearest neighbor pairs where at least one spin is not located at the surface.  $J_s$  resp.  $J_b$  is the strength of the surface resp. bulk couplings.

The surface phase diagram of the semi-infinite Ising model is well established. It is especially simple in two dimensions where surface and bulk order at the bulk critical temperature  $T_c$ , independently of the strength of the surface couplings. In three dimensions, however, different phase transitions are observed, depending on the value of  $J_s$ . For weak surface couplings order can not be maintained at the surface independently of the bulk. Consequently, surface and bulk both order at the bulk critical temperature. This transition is called ordinary transition. For strong surface couplings, however, with  $J_s > r_{sp} J_b$  where  $r_{sp} \approx 1.50$  for the simple cubic lattice,<sup>26,27</sup> the surface can order independently of the bulk at a temperature higher than  $T_c$ . Reducing the temperature the bulk than orders at  $T_c$  in presence of an already ordered surface (extraordinary transition). The different critical lines meet at the multicritical special transition point  $r_{sp}$ .

In our study of the nonequilibrium critical dynamics in Ising models with free surfaces we restricted ourselves to the ordinary transition and to the special transition point, thereby focusing on the short-time critical dynamics, the dynamical scaling regime encountered for longer times having been studied recently in Ref. 24 and 25. Table I lists the values of the static and dynamic bulk and surface exponents for the cases under investigation. For the ordinary transition we chose  $J_s = J_b$ , but some simulations were also done at other values of  $J_s$  to check for universality. As usual, the system was initially prepared in an uncorrelated state and then quenched to the critical temperature at time  $t = 0$ . The dynamical evolution of the system was studied using heat-bath dynamics. In two dimensions systems with typically  $300^2$  spins were simulated, whereas in three dimensions a typical sample contained  $60^3$  spins. Free surfaces were considered in one direction, whereas periodic boundary conditions were applied in the remaining directions. No finite-size effects were observed for the large systems under investigation.

## 2. Hilhorst-van Leeuwen model

The Hilhorst-van Leeuwen model is a two-dimensional semi-infinite Ising model with an extended surface defect.<sup>13,19</sup> We have studied this model on a square lattice. Whereas the couplings parallel to the surface have a constant strength  $J_1$ , the strength of the couplings perpendicular to the surface vary as a function of the distance  $y$  to the surface:

$$J_2(y) - J_2(\infty) = \frac{\tilde{A}}{y^\omega}. \quad (22)$$

with  $\tilde{A} = A T_c \sinh(2J_2(\infty)/T_c)/4$ .<sup>28</sup> In the present work only the marginal case with  $\omega = 1$  and  $J_1 = J_2(\infty)$  has been considered. For  $A < 1$  exact results show that the local scaling dimension  $x_1$  is a continuous function of  $A$  with

$$x_1 = \frac{1}{2}(1 - A). \quad (23)$$

This remarkable property allows us to study in a very systematic way the nonequilibrium dynamical behavior, passing from the domain growth regime to the cluster dissolution regime by only changing the value of the parameter  $A$ . Especially, for  $A = -0.06$  we have  $x_1 = x_i$ , whereas for  $A = 0$  we recover the pure semi-infinite model with  $x_1 = \frac{1}{2}$ . Of course, the nonequilibrium bulk quantities  $x_i$  and  $z$  are left unchanged by the presence of an extended surface defect.

## 3. Bariev model

The plane Ising model with a defect line is another inhomogeneous system displaying non-universal critical behavior. In his work Bariev<sup>13,20</sup> analyzed two types of defect lines: a chain defect, where a column of perturbed couplings with strength  $J_{ch}$  is considered, and a ladder defect, where modified couplings of strength  $J_l$  connect spins belonging to two neighboring columns (i.e. for  $J_l = 0$  the system is separated into two semi-infinite parts). The short-time nonequilibrium critical behavior has already been studied in systems with a chain defect.<sup>29</sup> In the present work we focus on Ising systems with a ladder defect.

Bariev's exact results demonstrate the dependence of the local scaling dimension  $x_l$  on the values of the defect coupling. For the ladder defect he obtains

$$x_l = \frac{2}{\pi^2} \arctan^2(\kappa_l^{-1}) \quad (24)$$

with

$$\kappa_l = \tanh\left(\frac{J_l}{T_c}\right) / \tanh\left(\frac{J}{T_c}\right). \quad (25)$$

$J$  is the strength of the unperturbed interactions (in the following we set  $J = 1$ ), whereas  $T_c$  is the critical temperature of the pure two-dimensional Ising model. Eq. (24)

shows that enhanced (reduced) defect couplings yield a lower (higher) local scaling dimension as compared to the perfect two-dimensional Ising model, the largest value being obtained for the semi-infinite model with  $J_l = 0$ . We therefore have always  $x_l < x_i$  in the case of a ladder defect and accordingly expect to encounter the domain growth regime for all values of the defect coupling.

As for the two-dimensional semi-infinite model and the Hilhorst-van Leeuwen model systems with the linear extent  $L = 300$  have been studied typically. For the Bariev model periodic boundary conditions are considered in all directions.

### B. Local magnetization relaxation

In order to study the relaxation of the magnetization the system is prepared in an initial state with a small magnetization  $m_i$ . In the actual simulations initial magnetizations  $m_i = 0.02$  and  $0.04$  were usually considered, for some selected cases other values of  $m_i$  were also investigated. The data shown in the different figures have been obtained after averaging over at least 60000 realizations using different random numbers and different initial states.

The relaxation of the local magnetization is shown in Figures 1 - 3 for the different models. Recall that depending on the values of  $x_l$  and  $x_i$  two different scenarios are possible. When cluster dissolution takes place ( $x_l > x_i$ ) scaling theory predicts a stretched exponential decay (6) at early times followed by a power-law decay at later times governed by the exponent  $\theta_l = (x_i - x_l)/z < 0$ . When  $x_l < x_i$ , however, the local magnetization should display a power-law increase with the exponent  $\theta_l = (x_i - x_l)/z > 0$ . Our data completely agree with this picture.

Looking at Table I we see that for the three-dimensional semi-infinite model  $x_l > x_i$  at the ordinary transition, whereas  $x_l < x_i$  at the special transition point and in the two-dimensional model. Accordingly, we expect the cluster dissolution process to take place only for the ordinary transition in the three-dimensional system. Figure 1 shows the relaxation of the surface magnetization for the pure semi-infinite systems. We first remark that at later times a power-law behavior is observed in all cases. The values of the exponent extracted in this regime are listed in Table II and compared with the expected theoretical value  $\theta_l = (x_i - x_l)/z$ . In all cases a nice agreement is found between the numerical value and the theoretical prediction. At early times the surface magnetization at the ordinary transition in three dimensions displays a nonalgebraic behavior. The exponent  $\kappa$  obtained from fitting the data with a stretched exponential (grey line) is listed in Table III. It nicely agrees with the scaling prediction (7).

The relaxation behavior of the surface magnetization is shown in Figure 2 for the Hilhorst-van Leeuwen model with various values of the scaling dimension  $x_1$ . Clearly,

TABLE II: Numerically determined values of the exponent  $\theta_l$  governing the power-law behavior of the local magnetization when starting from a state with a non-vanishing initial magnetization. The theoretical prediction is  $\theta_l = (x_i - x_l)/z$ . OT: ordinary transition, SP: special transition point.

pure semi-infinite models			
	$x_l$	numerical	theoretical
$d = 2$	1/2	0.015(3)	0.014
$d = 3$ , OT	1.26	-0.255(4)	-0.255
$d = 3$ , SP	0.376	0.179(4)	0.178
Hilhorst-van Leeuwen model			
$A$	$x_1$	numerical	theoretical
0.75	1/8	0.188(3)	0.187
0.50	1/4	0.131(3)	0.130
0.25	3/8	0.076(4)	0.072
-0.25	5/8	-0.045(2)	-0.044
-0.50	3/4	-0.107(4)	-0.101
-0.75	7/8	-0.157(3)	-0.159
-1	1	-0.214(5)	-0.217
-1.25	9/8	-0.29(1)	-0.274
-1.50	5/4	-0.37(3)	-0.332
Bariev model			
$J_l$	$x_l$	numerical	theoretical
0.2	0.376	0.072(1)	0.071
0.4	0.278	0.118(1)	0.116
0.6	0.208	0.148(1)	0.148
0.8	0.159	0.171(1)	0.171
1.0	0.125	0.188(1)	0.187
1.2	0.101	0.199(1)	0.198
1.4	0.085	0.208(2)	0.206

TABLE III: Numerically determined values of the exponent  $\kappa$  governing the stretched exponential behavior of the cluster dissolution process taking place when  $x_l > x_i$ . The values have been extracted from (I) the relaxation of the local magnetization and (II) from the short-time behavior of the single spin autocorrelation. The theoretical prediction is given by Eq. (7). OT: ordinary transition.

pure semi-infinite models				
	$x_l$	I	II	theoretical
$d = 3$ , OT	1.26	0.81(3)	0.81(2)	0.78
Hilhorst-van Leeuwen model				
$A$	$x_1$	I	II	theoretical
-0.25	5/8	0.11(4)	0.25(4)	0.19
-0.50	3/4	0.45(3)	0.41(3)	0.44
-0.75	7/8	0.71(3)	0.65(3)	0.69
-1	1	0.97(4)	0.89(3)	0.94
-1.25	9/8	1.17(4)	1.19(3)	1.19
-1.50	5/4	1.48(4)	1.54(5)	1.44

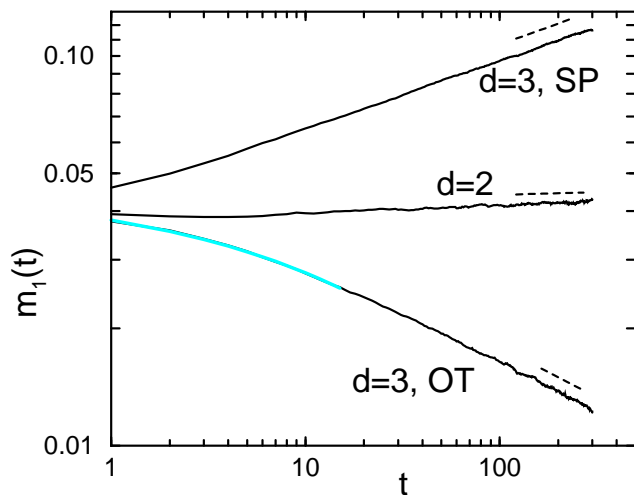


FIG. 1: Relaxation of the surface magnetization in the two- and the three-dimensional semi-infinite Ising models with  $m_i = 0.04$ . OT: ordinary transition, SP: special transition point. The grey line for the ordinary transition in three dimensions is a fit to the predicted stretched exponential behavior (6) at early times. The dashed lines indicate the power-law behavior taking place in the domain growth regime.

two different regimes are observed. For  $x_1 < x_i$  the magnetization increases, whereas for  $x_1 > x_i$  it decreases, the decrease being nonalgebraic at early times. The pure system  $x_1 = 1/2$  is very close to the borderline value 0.53 separating the two cases. This may explain the shallow minimum observed after the very first time steps before the magnetization increases again. In all cases a power-law behavior is encountered at later times, with an exponent that nicely agrees with the theoretical expectation, see Table II. The nonalgebraic decay in the cluster dissolution regime can in all cases be fitted by a stretched exponential. The values of the exponent  $\kappa$  extracted from these fits are listed in Table III. As for the three-dimensional Ising model at the ordinary transition we find a good agreement with the values obtained from the scaling theory.

Finally, Figure 3 is devoted to the two-dimensional Ising model with a ladder defect. As for all defect strengths  $J_l$  one has  $x_l < 1/2$ , the domain growth regime is the only one accessible within this model. Indeed, as shown in the Figure, we always observe an increasing magnetization. Again, the exponent extracted from these data perfectly agrees with the scaling prediction  $\theta_l = (x_i - x_l)/z$ . It has to be noted that the same agreement is obtained for a chain defect when comparing the theoretical prediction with the numerically determined values given in Ref. 29.

Before turning to the autocorrelation functions, let us briefly discuss the robustness of the exponents  $\theta_l$  and  $\kappa$  listed in Tables II and III. For this we investigated the ordinary transition in the pure semi-infinite systems by changing the strength of the surface couplings,  $J_s$ . One

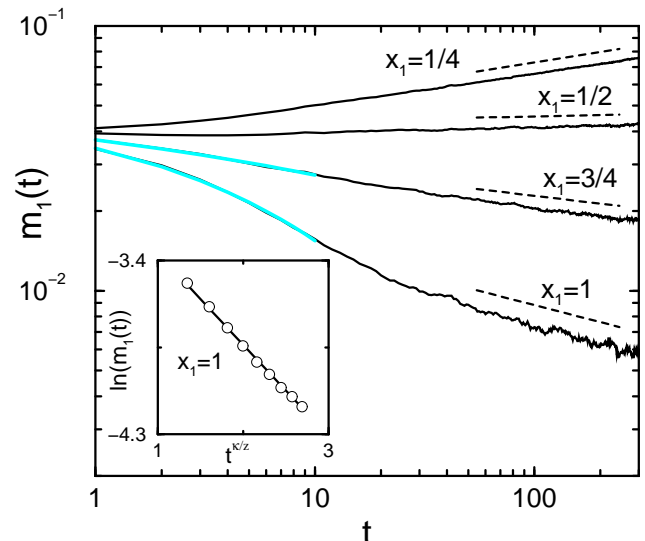


FIG. 2: Relaxation of the surface magnetization in the Hilhorst-van Leeuwen model for different values of the surface scaling dimension  $x_1$ . The value of the initial magnetization is  $m_i = 0.04$ . The grey lines for the cases  $x_1 > x_i \approx 0.53$  are obtained by fitting a stretched exponential to the early time data, see Eq. (6). The expected power-law behavior is indicated by the dashed lines. The inset shows that for  $x_1 = 1$   $\ln(m_1)$  is proportional to  $t^{\kappa/z}$  at early times, see Eq. (A.1), as expected for the cluster dissolution regime.

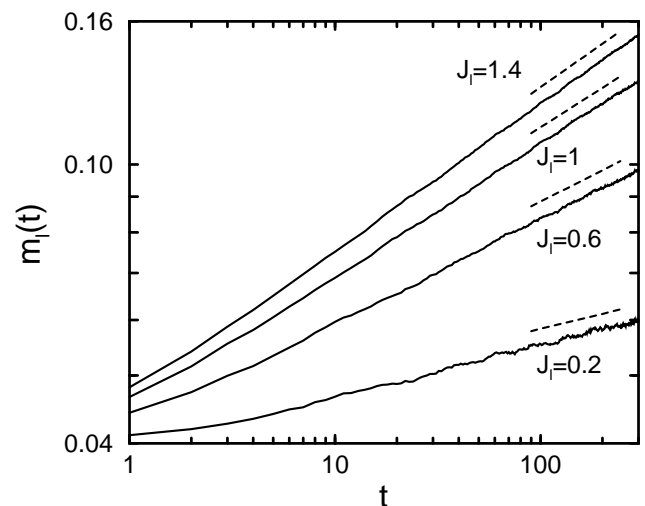


FIG. 3: Relaxation of the surface magnetization in the Bariev model for different strengths of the defect coupling  $J_l$ . The dashed lines indicate the expected power-law increase.

then observes that the value of  $\theta_l$  is very robust against modifications of the surface coupling strength. In all studied cases a power-law behavior with a constant  $\theta_l$  sets in when entering the domain growth regime. When dealing with the three-dimensional system, the cluster dissolution regime is encountered at early times, yielding a stretched exponential behavior, with a crossover to a



power-law at later times. It is this crossover time which is strongly affected by the strength of the surface couplings. For weak surface couplings, as for example for  $J_s = J_b/2$ , dissolution of clusters is extremely effective in the surface region, yielding a stretched exponential decay only at the very first time steps, the system crossing over to the DG regime very rapidly. This fact makes the extraction of  $\kappa$  in this case very tedious. On the other hand, when increasing the strength of the surface interactions, one approaches the special transition point located at  $J_s \approx 1.5J_b$ . As a result complicated crossover effects are encountered which again make a reliable determination of  $\kappa$  difficult. The value of  $\kappa$  reported in Table III has been obtained for  $J_s = J_b$  where the discussed effects are only of minor importance. Similar remarks also apply to the autocorrelation functions discussed in the following.

### C. Single spin autocorrelation function

Following Eq. (12) the CD process should lead to an unusual stationary behavior of the single spin autocorrelation at early times where  $t - s \ll s$ . In our simulations we calculated the local quantity

$$C(t, s) = \frac{1}{S} \sum_{i \in \text{surface}} \langle \sigma_i(t) \sigma_i(s) \rangle \quad (26)$$

with  $t > s$ , whereas  $S = L^{d-1}$  is the size of the surface or interface and  $L$  is the linear extent of the system. The average is done over at least 10000 different realizations of the thermal noise. The sum in (26) is over all spins belonging to the surface or to the defect plane. In the present study we restrict ourselves to the short-time regime with  $t - s \leq 300$ . The dynamical scaling regime  $t, s, t - s \gg 1$  has been analyzed in Ref. 24.

Our results for  $C(t, s)$  are summarized in Figures 4 and 5 and in Table III. In Figure 4 we plot  $C(t, s)$  versus  $t - s$  for the pure semi-infinite cases, whereas the same is done in Figure 5 in the Hilhorst-van Leeuwen model for two different values of the scaling dimension  $x_1$ . In case of a stationary autocorrelation at short times the different curves corresponding to different waiting times should be indistinguishable. This is exactly what is observed for the cases with a CD regime where  $x_1 > x_i$ . When  $x_1 < x_i$ , however, the single spin autocorrelation function is not stationary but depends in a more complicated way on both times  $t$  and  $s$  and not merely on the time difference  $t - s$ . In the CD regime we again observe a stretched exponential decay as predicted, see Eq. (12). This is illustrated in the inset of Figure 4a where we plot for the ordinary transition in three dimensions  $\ln(C(t, s))$  as a function of  $(t - s)^{\kappa/z}$ . Fitting a stretched exponential function to the short-time data we can extract the decay exponent  $\kappa$ . The resulting values are listed in Table III together with the estimates obtained from the relaxation measurements. A good agreement with the theoretical

prediction is observed.

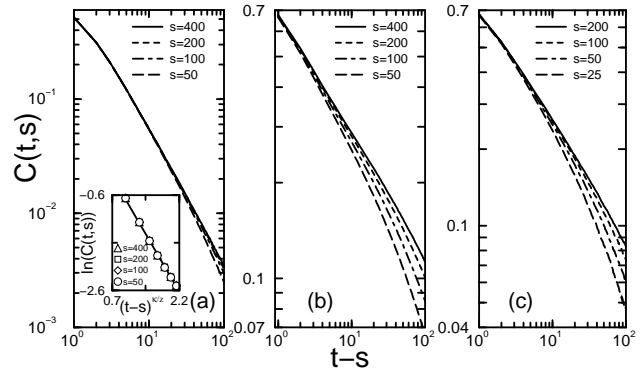


FIG. 4: Single spin autocorrelation vs the time difference  $t - s$  for different pure semi-infinite systems: (a) ordinary transition and (b) special transition point in three dimensions, and (c) ordinary transition in two dimensions. When  $x_1 > x_i$  a stationary behavior is observed with a stretched exponential decay at early times, see inset in (a). When  $x_1 < x_i$  the autocorrelation depends in a more complicated way on both times  $t$  and  $s$ .

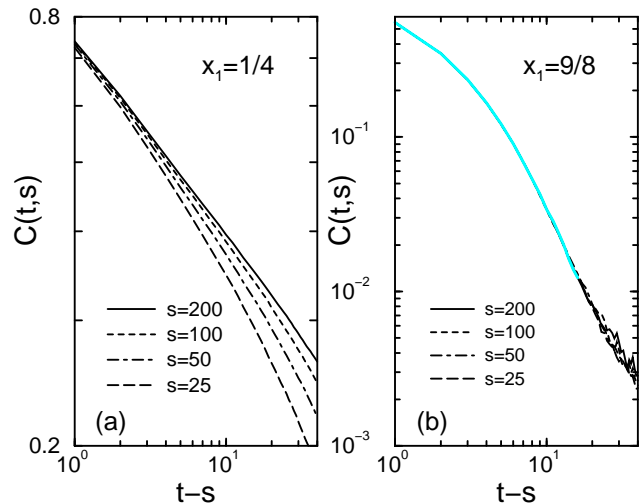


FIG. 5: Single spin autocorrelation as function of the time difference  $t - s$  as obtained for the Hilhorst-van Leeuwen model with different waiting times. A stationary behavior is observed in case (b) where  $x_1 > x_i$ . The grey line is obtained by fitting a stretched exponential to the short time data.

### D. Manifold autocorrelations

The phenomenological theory presented in Section II yields very remarkable predictions regarding the surface manifold autocorrelation function in an inhomogeneous critical system. For a surface or a defect plane in two dimensions the surface manifold  $\mathcal{M}$  has the dimensionality

$d' = 1$ , whereas  $d' = 2$  for a three-dimensional system. The surface manifold autocorrelation function is defined by

$$G_l(t, s) = \langle S(t) S(s) \rangle \quad (27)$$

with  $S(t) = \sum_{i \in \mathcal{M}} \sigma_i(t)$ , the sum extending over all spins belonging to the manifold.

For  $t = s$  scaling theory predicts a power-law increase of  $G_l(t, t)$  with an exponent  $(d' - x_l - x)/z$  whenever  $d' > x_l + x$ . When  $d' < x_l + x$ , however, the surface manifold autocorrelation function should rapidly tend to a constant. Recalling the possible values of  $x_l$  and  $x$  in the models under investigation, we see that for the pure semi-infinite models and for the Bariev model  $G_l(t, t)$  should display a power-law increase in all cases. Only in the Hilhorst-van Leeuwen model should one enter the regime with  $d' < x_l + x$ , with the amplitude value  $A = -0.75$  (i.e.  $x_1 = 7/8$ ) separating the two regimes. This limiting case  $x_1 = 7/8$  is shown in Figure 6a by the grey line. Indeed, a completely different behavior is observed for smaller values of  $x_1$  (lines above the grey line) when compared to larger values of  $x_1$  (lines below the grey line): in the former case  $G_1(t, t)$  increases with time whereas in the latter case  $G_1(t, t)$  rapidly saturates. In Figure 6b we compare the data with  $d' > x_l + x$  to the expected power-law increase. For all studied cases we find excellent agreement with scaling theory.

As noted in Section II scaling theory predicts for  $t > s$  in the DG regime with  $d' > x_l + x$  a change in the form of the short distance expansion of the surface manifold autocorrelation function as compared with that for  $t = s$ . Looking at Eqs. (18) and (19) one remarks that the scaling combination  $s^{(x_l - x)/z} G_1(t, s) / G_1(s, s)$  should then only be a function of  $t/s$ . As shown in Fig. 3 of Ref. 18 plotting this scaling combination as a function of  $t/s$  yields a perfect data collapse for different values of the local scaling dimension  $x_l$  and for different waiting times, thus demonstrating the expected  $t/s$  dependence.

On the other hand in the CD regime with  $d' < x_l + x$  the autocorrelation  $G_1(t, s)$  should just be a function of the time difference  $t - s$ , see Eq. (20). This stationary behavior is indeed observed, as shown in Figure 7 for the Hilhorst-van Leeuwen model with  $x_1 = 9/8$ . In the inset we verify the stretched exponential behavior (20) by plotting  $\ln(G_1)$  as a function of  $(t - s)^{\kappa'/z}$  for  $x_1 = 1$  and  $x_1 = 5/4$ . The values of  $\kappa'$  obtained by fitting the short time data with this kind of function are gathered in Table IV and compared with the theoretical expectation  $\kappa' = (x_1 - x)d/(d - 1)$ . For  $x_1 = 5/4$  we observe a simple exponential, in agreement with  $\kappa'/z > 1$ .

### E. Persistence of surface manifold

Finally, let us discuss the persistence of surface manifolds. The probability  $P_{pr}(t)$  that the manifold magnetization has not changed sign up to time  $t$  is of course directly related to the functional form of the surface

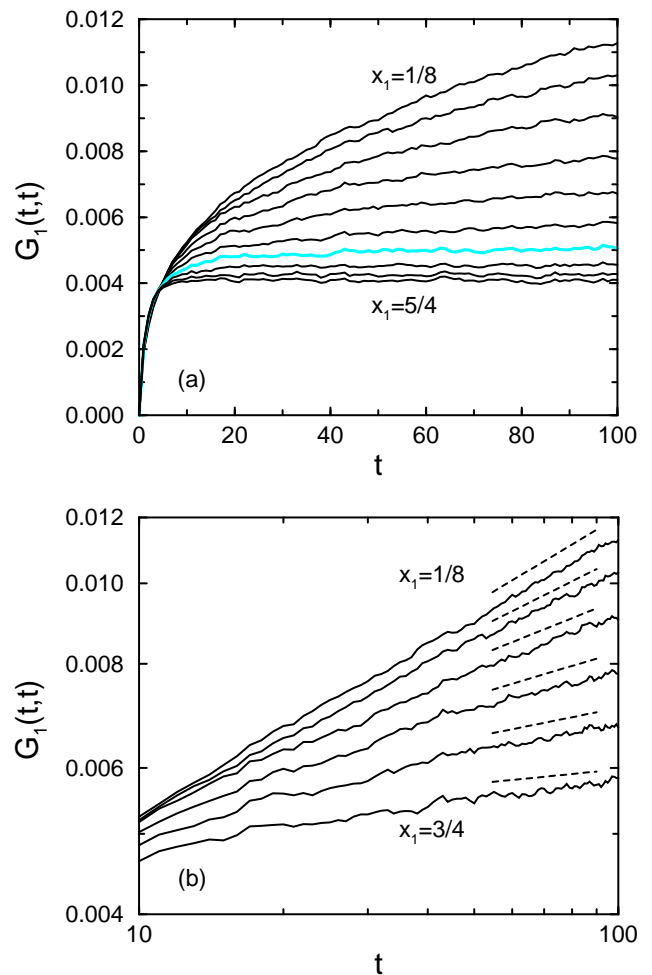


FIG. 6: (a) Surface manifold autocorrelation function for the Hilhorst-van Leeuwen model for various values of the scaling dimension:  $x_1 = i/8$  with  $i = 1, \dots, 10$  (from top to bottom). The grey line is obtained for  $x_1 = 7/8$  and separates the two different regimes with diverging  $G_1(t, t)$  for  $x_1 < 7/8$  and saturating  $G_1(t, t)$  for  $x_1 \geq 7/8$ . (b) Comparison of the increase of  $G_1(t, t)$  for  $x_1 < 7/8$  with the expected power-law (dashes lines) in a log-log plot. From top to bottom:  $x_1 = i/8$  with  $i = 1, \dots, 6$ .

manifold autocorrelation. Results for the CD regime are shown in Fig. 4 of Ref. 18. Plotting  $\ln(P_{pr})$  as function of  $t^{\kappa'/z}$  we observe straight lines that indicate that the probability is indeed governed by a stretched exponential decay whenever  $d' < x_l + x$ . Values obtained for  $\kappa'$  nicely agree with those obtained from the surface manifold autocorrelations, see Table IV. Figure 8 and Table V summarize our results for the DG regime with  $d' > x_l + x$ . The same behavior is observed in the different models: the probability  $P_{pr}(t)$  decays as a power of time. The values of the power-law exponent  $\Theta'_{pr}$  extracted from the numerical data are gathered in Table V. No theoretical expression for  $\Theta'_{pr}$  is available.

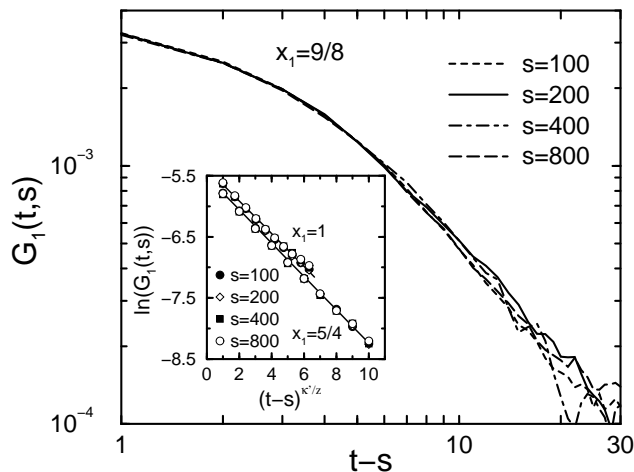


FIG. 7: Early time behavior of the surface manifold auto-correlation function in the CD regime as obtained for the Hilhorst-van Leeuwen model with  $x_1 = 9/8$ . In the inset the stretched (pure) exponential behavior is verified for two different values of  $x_1$ .

TABLE IV: Numerically determined values of the exponent  $\kappa'$  governing the stretched exponential behavior of the surface manifold autocorrelation function in the CD regime when  $d' < x_l + x$ . The values have been extracted from (I) the behavior of surface manifold autocorrelations and (II) from the decay of the persistence probability  $P_{pr}$ . The theoretical prediction is given by  $\kappa' = (x_1 - x)d/(d - 1)$ .

Hilhorst-van Leeuwen model				
$A$	$x_1$	I	II	theoretical
-0.75	7/8	1.41(2)	1.41(2)	1.41
-1	1	1.63(2)	1.61(2)	1.65
-1.25	9/8	1.86(2)	1.84(2)	1.88
-1.50	5/4	2.03(2)	2.03(2)	2.04

#### IV. DISCUSSION

Nonequilibrium critical dynamics involves a time horizon, where the quench to the critical temperature is made, and this has a long-time, scale-free effect on the dynamical processes in the system. New nonequilibrium exponents enter into the theory: the relaxation of the magnetization and the spin-spin (and manifold) auto-correlations involve the scaling dimension of the initial magnetization,  $x_i$ , whereas persistence of different manifolds involve a new exponent  $\Theta_{pr}$ . In a spatially inhomogeneous system, such as at a free surface or at a defect plane, the local critical behavior is generally different from that in the bulk and one has to introduce local critical exponents, such as  $x_l$  for the local magnetization. In this paper we studied nonequilibrium critical phenomena in inhomogeneous systems, in which the dynamical behavior is the result of an interplay between a spatial and a temporal inhomogeneity. Our main result is that in

TABLE V: Numerically determined values of the manifold persistence exponent  $\Theta'$  governing the power-law decay of the persistence probability  $P_{pr}(t)$  in the domain growth regime. OT: ordinary transition, SP: special transition point.

pure semi-infinite models		
	$x_1$	$\Theta'$
$d = 2$	1/2	3.0(2)
$d = 3$ , OT	1.26	4.6(3)
$d = 3$ , SP	0.376	0.61(2)
Hilhorst-van Leeuwen model		
$A$	$x_1$	$\Theta'$
0.75	1/8	0.97(2)
0.50	1/4	1.63(3)
0.25	3/8	2.0(2)
-0.25	5/8	3.9(3)
-0.50	3/4	4.5(3)
Bariev model		
$J_l$	$x_l$	$\Theta'$
0.2	0.376	2.3(1)
0.4	0.278	1.75(5)
0.6	0.208	1.27(3)
0.8	0.159	0.90(2)
1.0	0.125	0.71(2)
1.4	0.085	0.55(1)
1.8	0.064	0.40(2)

such a system in early times two types of nonequilibrium processes can take place. Conventional domain growth phenomena is observed if the temporal surface is more disordered, than the spatial one. This is the rule in the bulk of the system. There is, however, a second, up to now unnoticed process: when the spatial surface is more disordered than the temporal one, then in early times local order is reduced and cluster dissolution takes place. This process is manifested by fast, stretched exponential relaxation and by stationary, stretched exponential autocorrelations, which, however, involve a universal exponent. We have shown by scaling theory and checked by numerical calculations that as far as relaxation and autocorrelations are concerned the local nonequilibrium processes can be fully characterized by the existing exponents,  $x_l$ ,  $x_i$  and by the dynamical exponent,  $z$ , both in the DG and in the CD regimes.

Our results can be applied or generalized to other types of systems. We mention that the cluster dissolution scenario has recently been noticed in nonequilibrium relaxation of reaction-diffusion systems, such as the contact process.<sup>30</sup> For another type of inhomogeneous systems<sup>13,14</sup> we mention inhomogeneities of geometrical origin, such as wedges, corners and cones. For example the local exponent at a corner,  $x_c$ , depends on the opening angle,<sup>13,31</sup>  $\varphi$ , and in two dimensions it is related to the surface exponent as  $x_c = x_1\pi/\varphi$  through conformal invariance.<sup>32</sup> Generally local order at a corner is weaker

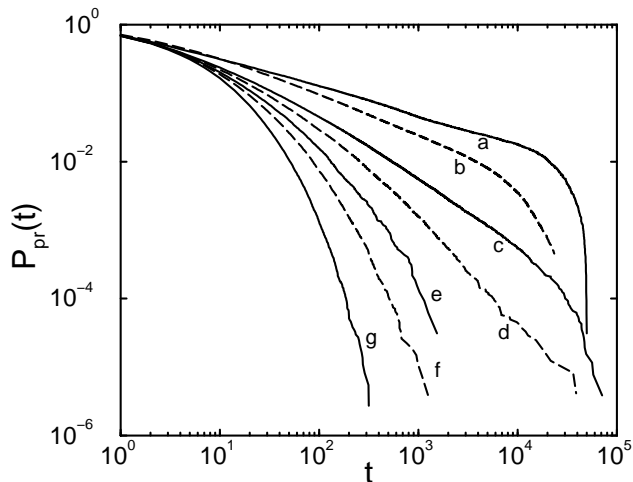


FIG. 8: Manifold persistence probability  $P_{pr}(t)$  as a function of  $t$  in the domain growth regime for various cases. a: defect line persistence in the Bariev model with  $J_l = 1.8$ , b: surface persistence in the three-dimensional semi-infinite model at the special transition point, c: surface persistence in the Hilhorst-van Leeuwen model with  $A = 0.75$ , d: surface persistence in the Hilhorst-van Leeuwen model with  $A = 0.50$ , e: defect line persistence in the Bariev model with  $J_l = 0.4$ , f: surface persistence in the pure semi-infinite two-dimensional Ising model, g: surface persistence in the three-dimensional semi-infinite model at the ordinary transition.

than at a free surface, therefore one expects that the cluster dissolution scenario often applies for such systems.

### Acknowledgments

We thank the Regionales Rechenzentrum Erlangen for the extensive use of the IA32 compute cluster. This work has been supported by the Hungarian National Research Fund under grant No OTKA TO34183, TO37323, TO48721, MO45596 and M36803.

### APPENDIX: NONEQUILIBRIUM DYNAMICS WITH CLUSTER DISSOLUTION

Nonequilibrium dynamics of inhomogeneous systems, in which the local (surface) scaling dimension,  $x_l$ , is larger than the scaling dimension of the initial magnetization,  $x_i$ , is governed by cluster dissolution (CD).<sup>18</sup> (Similar scenario holds for the surface manifold autocorrelation function for  $d' < x_l + x$ .) In this case the nonequilibrium growth process, which goes in time as  $\sim t^{x_i/z}$ , is much weaker than critical local relaxation, which has a time dependence of  $t^{-x_l/z}$ . As a result typically no ordered domains are created in the surface region and the dynamics is governed by large correlated clusters which are present with a very small probability in the initial state.

### 1. Relaxation

Let us start with an initial state having a magnetization,  $m_i$ . The probability of having a cluster of linear size,  $l$ , is given by  $P(l) \sim m_i^d$ , where  $d$  is the dimension of the system. During the relaxation process the mass of a cluster is diluted by a factor of  $t^{(x_i-x_l)/z}$ , and the cluster is dissolved, if a domain wall of size  $l^{d-1}$  is created in it. From the relation  $t(l)^{(x_i-x_l)/z} l^{d-1} = O(1)$  we obtain for the typical time-scale of a cluster of linear size,  $l$ :  $t(l) \sim l^{(d-1)z/(x_i-x_l)}$ . After time  $t > t(l)$  only those clusters exist, which have an original size larger than  $l$ . The magnetization,  $m(t)$ , is just given by the contribution of these large clusters:  $m(t) \sim \sum_{l>t(l)} P(l)l^d$ . From this we obtain in leading order:

$$\ln(m(t)/m_i) \sim -t^{\kappa/z}, \quad \kappa = \frac{(x_l - x_i)d}{(d-1)}. \quad (\text{A.1})$$

Note, however, that the relaxation can not be faster, than in the *non-critical case*, when it is pure exponential, i.e. the exponent in Eq.(A.1) reads as:  $\min(\kappa/z, 1)$ . This result is compatible with the scaling form in Eq.(6) and (7).

### 2. Single spin autocorrelations

The reasoning is similar as for relaxation and we repeat that for a completely uncorrelated initial state with zero magnetization the probability of having a large cluster of linear size,  $l$ , is given by  $P(l) \sim \exp(-Al^d)$  and the corresponding relaxation time is  $t_r = t(l) \sim l^{(d-1)z/(x_l-x_i)}$ . The autocorrelation function is obtained by performing an average over the clusters:

$$C(\tau) \sim \int P(t_r) \exp(-\tau/t_r) dt_r \sim \exp(-C\tau^{\kappa/z}), \quad (\text{A.2})$$

in terms of  $\tau = t - s < s$ . If it happens that  $\kappa/z > 1$ , then the decay is pure exponential. Note that the autocorrelation function is stationary for early times and is compatible with Eq.(12).

### 3. Manifold autocorrelations

For surface manifold autocorrelations the regime of cluster dissolution is valid for  $d' < x_l + x$ . In this case the dilution of ordered clusters goes in time as  $t^{(x-x_l)/z}$ . As a consequence results for the single spin autocorrelation function can be easily translated, just in Eq.(A.2) the decay exponent  $\kappa$  has to be replaced by  $\kappa' = (x_l - x)d/(d-1)$ . The corresponding results are in Eq.(20).

- 
- <sup>1</sup> P.C. Hohenberg and B.I. Halperin, *Rev. Mod. Phys.* **49**, 435 (1977).
- <sup>2</sup> H.K. Janssen, B. Schaub, and B. Schmittmann, *Z. Phys.* **B73**, 539 (1989).
- <sup>3</sup> D. Huse, *Phys. Rev.* **B40**, 304 (1989).
- <sup>4</sup> H.K. Janssen, *From Phase Transition to Chaos*, eds. G. Györgyi, I. Kondor, L. Sasvári and T. Tél, *Topics in Modern Statistical Physics* (World Scientific, Singapore, 1992).
- <sup>5</sup> S.N. Majumdar and A.J. Bray, *Phys. Rev. Lett.* **91**, 030602 (2003).
- <sup>6</sup> S.N. Majumdar, *Curr. Sci. India* **77**, 370 (1999), and *cond-mat/9907407*.
- <sup>7</sup> S.N. Majumdar, A.J. Bray, S.J. Cornell, and C. Sire, *Phys. Rev. Lett.* **77**, 3704 (1996).
- <sup>8</sup> A.J. Bray, *Adv. Phys.* **43**, 357 (1994).
- <sup>9</sup> C. Godrèche and J.M. Luck, *J. Phys. Cond. Matt.* **14**, 1589 (2002).
- <sup>10</sup> A. Crisanti and F. Ritort, *J. Phys. A: Math. Gen.* **36**, R181 (2003).
- <sup>11</sup> K. Binder, in *Phase Transitions and Critical Phenomena*, edited by C. Domb and J.L. Lebowitz (Academic Press, London, 1983), Vol. 8.
- <sup>12</sup> H.W. Diehl in *Phase Transitions and Critical Phenomena*, edited by C. Domb and J.L. Lebowitz (Academic Press, London, 1986, Vol. 10; H.W. Diehl, *Int. J. Mod. Phys. B* **11**, 3503 (1997).
- <sup>13</sup> F. Iglói, I. Peschel, and L. Turban, *Adv. Phys.* **42**, 683 (1993).
- <sup>14</sup> M. Pleimling, *J. Phys. A* **37**, R79 (2004).
- <sup>15</sup> S. Dietrich and H.W. Diehl, *Z. Phys. B* **51**, 343 (1983).
- <sup>16</sup> U. Ritschel and P. Czermer, *Phys. Rev. Lett.* **75**, 3882 (1995).
- <sup>17</sup> S.N. Majumdar and A.M. Sengupta, *Phys. Rev. Lett.* **76**, 2394 (1996).
- <sup>18</sup> M. Pleimling and F. Iglói, *Phys. Rev. Lett.* **92**, 145701 (2004).
- <sup>19</sup> H.J. Hilhorst and J.M. van Leeuwen, *Phys. Rev. Lett.* **47**, 1188 (1981).
- <sup>20</sup> R.Z. Bariev, *Sov. Phys. JETP* **50**, 613 (1979).
- <sup>21</sup> M. Kikuchi and Y. Okabe, *Phys. Rev. Lett.* **55**, 1220 (1985).
- <sup>22</sup> H. Riecke, S. Dietrich, and H. Wagner, *Phys. Rev. Lett.* **55**, 3010 (1985).
- <sup>23</sup> G.F. Newell and M. Rosenblatt, *Ann. Math. Stat.* **33**, 1306 (1962).
- <sup>24</sup> M. Pleimling, *Phys. Rev. B* **70**, 104401 (2004).
- <sup>25</sup> P. Calabrese and A. Gambassi, *cond-mat/0410357*.
- <sup>26</sup> K. Binder and D.P. Landau, *Phys. Rev. Lett.* **52**, 318 (1984).
- <sup>27</sup> C. Ruge, A. Dunkelmann, and F. Wagner, *Phys. Rev. Lett.* **69**, 2465 (1992).
- <sup>28</sup> H.W.J. Blöte and H.J. Hilhorst, *Phys. Rev. Lett.* **51**, 2015 (1983).
- <sup>29</sup> C.S. Simões and J.R. Drugowich de Felício, *J. Phys. A* **31**, 7265 (1998); T. Tomé, C.S. Simões and J.R. Drugowich de Felício, *Mod. Phys. Lett. B* **15**, 1141 (2001).
- <sup>30</sup> T. Enss, M. Henkel, A. Picone, and U. Schollwöck, *J. Phys. A* **37**, 10479 (2004); J.J. Ramasco, M. Henkel, M.A. Santos, and C. A. da Silva Santos, *J. Phys. A* **37**, 10497 (2004).
- <sup>31</sup> J.L. Cardy, *J. Phys. A* **16**, 3617 (1983).
- <sup>32</sup> J.L. Cardy, *Nucl. Phys. B* **240** [FS12], 514 (1984).